
# Therapeutic effect and mechanism study of *L*-cysteine derivative 5P39 on LPS-induced acute lung injury in mice

Yanting He, Yalei Zhao, Yuchen Feng, Anqi Ren, Yunyi Zhang, Yang Wang, Hong Li

PII: S0014-2999(19)30845-3

DOI: https://doi.org/10.1016/j.ejphar.2019.172893

Reference: EJP 172893

To appear in: *European Journal of Pharmacology*

Received Date: 2 September 2019

Revised Date: 11 December 2019

Accepted Date: 20 December 2019

Please cite this article as: He, Y., Zhao, Y., Feng, Y., Ren, A., Zhang, Y., Wang, Y., Li, H., Therapeutic effect and mechanism study of *L*-cysteine derivative 5P39 on LPS-induced acute lung injury in mice, *European Journal of Pharmacology* (2020), doi: https://doi.org/10.1016/j.ejphar.2019.172893.

HL and YW funded the study; YW and YLZ designed and synthesized compound **5P39**; HL, YYZ and YTH conceived and designed the experiments; YTH, YCF and AQR performed the *in vitro* and *in vivo* experiments; YTH and YLZ wrote the original draft; HL, YW and YYZ revised the manuscript. All authors reviewed the manuscript.

# Therapeutic effect and mechanism study of *L*-cysteine derivative 5P39 on LPS-induced acute lung injury in mice

Yanting He[a,1], Yalei Zhao[b,1], Yuchen Feng[a], Anqi Ren[a], Yunyi Zhang[a], Yang Wang[b,*], Hong Li[a,*]

[a]*Department of Pharmacology,* [b]*Department of Medicinal Chemistry, School of Pharmacy, Fudan University, Shanghai 201203, China*

[1]These authors contributed equally to this work.

[*]Corresponding authors. E-mail addresses: lxzhang@shmu.edu.cn (H. Li); wangyang@shmu.edu.cn (Y. Wang).



## ABSTRACT

Organosulfur compounds, such as *L*-cysteine, allicin and other sulfur-containing organic compounds in *Allium* species, have been proposed to possess many important physiological and pharmacological functions. A novel *L*-cysteine derivative, *t*-Butyl *S*-allylthio-*L*-cysteinate (**5P39**), was designed and synthesized by combining *L*-cysteine derivative and allicin pharmacophore through a disulfide bond. This study aimed to explore the effects and mechanisms of **5P39** on lipopolysaccharide (LPS)-induced acute lung injury (ALI) in mice. At the experimental concentration (5, 10 and 20 μM), **5P39** suppressed the excessive secretion of nitric oxide (NO) and interleukin-6 (IL-6) in mice peritoneal macrophages stimulated by LPS. A mouse model of ALI was established by tracheal instillation of LPS for 2 h before **5P39** (30 and 60 mg/kg) administration. The results showed that **5P39** treatment down-regulated the wet/dry weight ratio (W/D ratio) of lungs and reduced the protein concentration, the number of total cells as well as the myeloperoxidase (MPO) activity in bronchoalveolar lavage fluid (BALF). **5P39** administration improved the histopathological changes of lungs in ALI mice with the decreased levels of

pro-inflammatory cytokines in BALF. The inhibitory effects of **5P39** on the toll-like receptor 4 (TLR4) expression and macrophages accumulation in lung tissues were observed by immunohistochemistry. Additionally, **5P39** significantly attenuated the LPS-activated high expression of key proteins in TLR4/MyD88 signaling pathway. Taken together, the present study showed that **5P39** effectively alleviate the severity of ALI, and its mechanism might relate to the inhibition of LPS-activated TLR4/MyD88 signaling pathway, demonstrating a promising potential for further development into an anti-inflammatory drug candidate.

**Keywords**: *t*-Butyl *S*-allylthio-*L*-cysteinate; Acute lung injury; Lipopolysaccharide; Inflammation; Macrophages; Toll-like receptor 4

## 1. Introduction

Acute lung injury (ALI) is an inflammatory disease with high morbidity and mortality (Ye et al., 2019). ALI or its more severe form, acute respiratory distress syndrome (ARDS), is characterized by severe pulmonary edema, pneumonic cell aggregation and excessive production of inflammatory cytokines, leading to a strong pulmonary inflammatory response (Xu et al., 2015; Matthay et al., 2017). Epidemiological study has reported that ALI remains an important public health issue worldwide and a major challenge for clinicians (Bellani et al., 2016). Although some therapeutic strategies have been taken to improve functional outcomes, the mortality in ALI patients remains high (Wang et al., 2019b). Therefore, there is an urgent need to study the underlying mechanisms and novel therapeutic methods of ALI.

LPS is a major component of the cell wall of Gram-negative bacteria and has been widely used to establish experimental models for ALI drug development (Yao et al., 2017). The TLR family is the most important subgroup of pathogen recognition receptors (PRRs) (Pandey et al., 2019). Toll-like receptor 4 (TLR4), as the most primary response receptor of LPS (Zhou et al., 2019), is one of the important members of the TLR family.

LPS activates TLR4, and then induces phosphorylation of nuclear transcription

factor-κB (NF-κB) via the adaptor protein (myeloid differentiation factor 88, MyD88) and ubiquitin ligase (tumor necrosis factor receptor-associated factor 6, TRAF6) (Xia et al., 2019). Subsequently, pro-inflammatory cytokines such as tumor necrosis factor-α (TNF-α), interleukin-1β (IL-1β) and interleukin-6 (IL-6) were expressed in large amounts (Xia et al., 2019; Liu et al., 2019). These inflammatory mediators initiate and amplify the inflammatory response and then cause lung injury (Zhang et al., 2014; Zhou et al., 2016).

Recently, ample publications (Kashfi and Olson, 2013; Song et al., 2014; Zheng et al., 2017 and references therein) have probed organosulfur compounds, such as *L*-cysteine, methionine, allicin and other sulfur-containing organic compounds in *Allium* species (Fig. 1A), which have been proposed to possess many important physiological and pharmacological functions. *L*-cysteine derivative *S*-propargyl-cysteine was reported exerting anti-inflammatory (Gong et al., 2011) and anti-oxidative effects (Pan et al., 2012). *S*-allylmercaptocysteine showed protective effect on cisplatin nephrotoxicity (Zhu et al., 2017). Miron synthesized *S*-allylthio-captopril (CPSSA) by combining captopril with allicin through a disulfide bond, and the study of its biological effect proved that CPSSA not only possessed the advantages of both captopril and allicin, but also showed more potent antihypertensive effect than captopril through synergic effect (Miron et al., 2004; Miron et al., 2010). In our previous study, a series of conjugates of Danshensu-cysteine derivatives were reported to exert significant cytoprotective effects by anti-oxidative and anti-apoptotic activities (Dong et al., 2009; Jia et al., 2012; Pan et al., 2013; Liu et al., 2013; Seetapun et al., 2013; Pan et al., 2015; Ren et al., 2018).

In a continuing effort to identify the bioactivities of these sulfur-containing organic compounds, *tert*-butyl *S*-allylthio-*L*-cysteinate (**5P39**, Fig. 1B) was designed and synthesized by conjugating *L*-cysteine derivative and allicin pharmacophore through a disulfide bond based on the combination principles. In this work, **5P39** demonstrated to be a promising potential anti-inflammatory agent with a mechanism related to the inhibition of LPS-activated TLR4/MyD88 signaling pathway.

## 2. Materials and Methods

### *2.1. Chemical synthesis of **5P39***

Target compound **5P39** was prepared via the synthetic route described in Fig. 1B. The oxidation of diallyl disulfide (**1**) with 30% $H_2O_2$ afforded allicin (**2**), which followed by reaction with *L*-cysteine hydrochloride to give *S*-allylthio-*L*-cysteine (**3**) in 90% yield for two steps. Compound **3** was then converted into **5P39** by transesterification reaction with *tert*-butyl acetate in the presence of $HClO_4$ in 24% yield, and byproduct **4** was obtained meanwhile in yield of 12%.

To a rapidly stirred solution of compound **1** (973 mg, 6.65 mmol) in acetic acid (4.0 ml) was added dropwise a mixture of 30% hydrogen peroxide (1.0 ml, 9.81 mmol) in acetic acid (3.0 ml) during 0.2 h at 0 □ . Then the mixture was continually stirred at 0 □ for 2 h and at r.t. for 4 h, and poured into ice-water (50 ml). The mixture was extracted with $CH_2Cl_2$ (4 × 50 ml), and the combined organic solvent was washed with saturated aqueous $Na_2CO_3$ solution (3 × 50 ml), dried over anhydrous $Na_2SO_4$, filtered and concentrated to give a residue (1.08 g) of crude product **2**. To a solution of the residue (450 mg) in water (40 ml) was added *L*-cysteine hydrochloride (2.0 g, 12.7 mmol) and enough sodium bicarbonate to adjust pH 6. White precipitate appeared immediately and was filtered after standing for 0.33 h, and then washed with water and ether successively to give a white solid. The obtained white solid was dissolved in 9% HCl (aq.) and extracted with ether. To the aqueous layer was added $NaHCO_3$ to adjust pH 6 and white solid precipitated out. The white solid was filtered, washed with water and ether, and dried to give compound **3** (480 mg, 90% for two steps) as a white powder, mp: 187-190 □ (Freeman et al., 1994. mp: 198-199 □).

To a rapidly stirred solution of compound **3** (3.49 g, 18.0 mmol) in *t*-butyl acetate (36 ml, 268 mmol) at 0 □ was slowly added $HClO_4$ (1.53 ml, 26.8 mmol). The mixture was stirred at room temperature for 12 h then adjusted to pH 9 by 10 % $Na_2CO_3$ (aq.), and then extracted with $CH_2Cl_2$ (3 × 100 ml). The combined organic solvent was dried over anhydrous $Na_2SO_4$, filtered and concentrated to give an oil. Silica gel flash column chromatography using $CH_2Cl_2$ as the eluent gave *t*-butyl *S*-allylthio-*L*-cysteinate (**5P39**, 1.10 g, 24%) and *t*-butyl *S*-(*t*-butyl)-*L*-cysteinate (**4**,

0.50 g, 12 %) as pale yellow oil respectively. Compound **5P39**: $^{1}$H NMR (400 MHz, $CDCl_3$) $\delta$ 5.80-5.95 (m, 1H), 5.25-5.16 (m, 2H), 3.69-3.66 (m, 1H), 3.35 (d, $J$ = 7.3 Hz, 2H), 3.10 (dd, $J$ = 13.4, 4.5 Hz, 1H), 2.84 (dd, $J$ = 13.4, 8.0 Hz, 1H), 1.48 (s, 9H). $^{13}$C NMR ($CDCl_3$, 100 MHz) $\delta$ 172.3, 132.7, 118.1, 81.1, 53.8, 43.7, 41.6, 27.4. ESI-MS *m/z*: 250.1 ($M + H^+$). Compound **4**: $^{1}$H NMR (400 MHz, $CDCl_3$) $\delta$ 3.54 (dd, $J$ = 7.4, 4.5 Hz,1H), 2.83 (ddd, $J$ = 19.7, 12.3, 5.9 Hz, 2H), 1.48 (s, 9H), 1.33 (s, 9H); ESI-MS (*m/z*): 234.2 ($M + H^+$).

*2.2. Reagents and antibodies*

LPS (Escherichia coli 055: B5), dexamethasone (DEX, used as the positive control in the *in vitro* experiments) and 3-(4,5-dimethyl-2-thiazolyl) -2,5-diphenyl-2-H-tetrazolium bromide (MTT) were purchased from Sigma–Aldrich (St. Louis, MO, USA). Fetal bovine serum (FBS) and RPMI-1640 medium were purchased from Biological Industries (Kibbutz Beit-Haemek, Israel). Diaminobenzidine (DAB) assay kit was purchased from Zhongshan Jinqiao Biotechnology Co., Ltd (Beijing, China). Dexamethasone sodium phosphate injection (DEX, used as the positive control in LPS-induced ALI model) was purchased from Chongqing Laimei Pharmaceutical Co., Ltd. (Chongqing, China). The enhanced bicinchoninic acid (BCA) protein assay kit and horseradish peroxidase (HRP)-conjugated IgG were purchased from Beyotime (Jiangsu, China). Enzyme-linked immunosorbent assay (ELISA) kits for mouse IL-6, TNF-α and IL-1β detection were purchased from Boatman Biotechnology Co., Ltd. (Shanghai, China). Myeloperoxidase (MPO) determination kit was purchased from Nanjing Jiancheng Bioengineering Institute (Jiangsu, China). Antibody specific to inducible nitric oxide synthase (iNOS) was purchased from Cell Signaling Technology (Danvers, MA, USA). Antibodies specific to TLR4, F4/80, MyD88, TRAF6, phospho-nuclear factor-κB p65 (p-NF-κB p65), β-actin were purchased from Abcam (Cambridge, UK). Antibodies specific to NF-κB p65 were purchased from Shanghai Abways Biotechnology Co., Ltd (Shanghai, China). Other reagents used in Western blot were purchased from Beyotime (Jiangsu, China).

*2.3. Animals and ethics statement*

Male BALB/c mice (14-18g) were purchased from Shanghai Slaccas Laboratory Animal Co., Ltd. (SPF II Certificate; No. SCXK2017-0005) and housed in the SPF Laboratory Animal Room with a 12 h light/dark cycle.

All animals received humane care in accordance with the "Guide for the Care and Use of Laboratory Animals" published by the National Institutes of Health. All animal experiments were approved by the Animal Ethical Committee of School of Pharmacy, Fudan University (No. 2018-03-YL-LH-01).

*2.4. Effect of **5P39** in vitro*

*2.4.1. Harvest and culture of peritoneal macrophages*

Male BALB/c mice were intraperitoneally injected with 1 ml of 5% sodium thioglycollate medium to activate peritoneal macrophages. Mice were killed 5 days after injection to harvest peritoneal macrophages. These cells were adjusted to $1\times10^6$ cells/ml with 10% FBS-RPMI-1640 and cultured at 200 μl/well in a 96-well plate. The cells used for experiment were divided into 10 groups including normal group , **5P39** (5, 10, 20 μM) group, DEX (10 μM) group, LPS (1 μg/ml) group, LPS (1 μg/ml) + **5P39** (5, 10, 20 μM) group, and LPS (1 μg/ml) + DEX (10 μM) group. The DEX-treated groups were taken as positive control.

Peritoneal macrophages were cultured at 37 □ in a humidified atmosphere containing 5% $CO_2$. The whole experiment procedures were carried out in aseptic conditions and all materials were previously sterilized and pyrogen-free (Xu et al., 2015; Wu et al., 2013).

*2.4.2. Detection of cell viability and inflammatory mediators*

Peritoneal macrophages were treated by **5P39** with or without LPS stimulation for 24 h, and the culture supernatants were collected for detection. Then culture mediums containing 0.5 mg/ml MTT were added to the wells. After 4 h of incubation, the mediums were discarded and the formazan crystals generated by the action of mitochondrial enzymes in viable cells were dissolved in dimethyl sulfoxide (DMSO). The absorbance of each well was measured at 570 nm using a microplate reader (Wu et al., 2013). The change of absorbance measured by the MTT method reflected the effect of **5P39** on cell activity.

Nitric oxide (NO) production in the peritoneal macrophages was detected by the Griess reagent to test its end product, nitrite (Wu et al., 2013). Griess reagent contained a mixture of equal volume of 0.1% *N*-(1-naphthyl) ethylenediamine dihydrochloride in $H_2O$ and 1% sulfanilamide in 5% $H_3PO_4$. Briefly, 50 μl culture supernatant collected previously was mixed with 50 μl Griess reagent in a 96-well plate. The absorbance was tested at 540 nm. The concentration of nitrite was determined according to a standard curve formed with sodium nitrite.

IL-6 production in the peritoneal macrophages was tested by mouse IL-6 ELISA kit according to the manufacturer's instructions.

*2.4.3. Culture of Ana-1 cell*

Ana-1 cells were obtained from ATCC (ATCCPTA-2662, Manassas, VA), which was a continuous cell line of murine macrophages. The cells in this experiment were adjusted to $2\times10^6$ cells/ml with 10% FBS-RPMI-1640 and cultured at 1 ml/well in a 6-well plate. These cells were divided into 3 groups including normal group, LPS (0.5 μg/ml) group and **5P39** (20 μM) group. The culture conditions of Ana-1 cells were similar to peritoneal macrophages in section 2.4.1. The cells treated by LPS with or without **5P39** administration for 30 min or 24 h were collected for Western blot analysis (in section 2.10).

*2.5. Experimental design of Animals*

Male BALB/c mice were randomly divided into 5 groups (n = 6): Sham-operated animals group (sham group), LPS (3 mg/kg) stimulated group (model group), LPS (3 mg/kg) + **5P39** group (**5P39** 30 mg/kg group and **5P39** 60 mg/kg group), and LPS (3 mg/kg) + DEX (4 mg/kg) group. The doses of LPS and drugs were determined based on our previous experiments and preliminary results.

**5P39** was ground and dissolved in PEG400. Then the **5P39** solution was diluted with 1% carboxymethylcellulose sodium (CMC-Na) and administered intragastrically (i.g.). LPS was dissolved in sterilized normal saline (NS). The model of ALI was established as previously described (Xu et al., 2015; Xie et al., 2013). The mice were anesthetized with 20% urethane (1 g/kg) before intratracheal instillation of NS (sham group, i.t.) or LPS (i.t.). 2 h after NS or LPS treatment, mice were administrated with

vehicle (1% CMC-Na-5% PEG400, i.g.), **5P39** (i.g.), or DEX (tail vein, i.v.). The mice in sham group and model group were given vehicle intragastrically.

Mice were killed 24 h after LPS instillation. Superior lobe of left lung was used to collect bronchoalveolar lavage fluid (BALF), which was flushed four times with 0.5 ml NS. The BALF from each sample was centrifuged to isolate the cells. The supernatant was collected for subsequent analysis of protein, MPO, and pro-inflammatory cytokines, while the total cells were gathered and resuspended in 100 μl 0.01 mol/L phosphate buffered saline (0.01 M PBS, pH 7.4) for cell counts. Inferior lobe of left lung and middle lobe of right lung were stored at -80 □ for subsequent analysis. Superior lobe of right lung was taken for histopathologic examination. Inferior lobe of right lung of mice was separated and weighed for wet/dry weight ratio (W/D ratio) count.

*2.6. Histopathologic evaluation of lung tissues*

The superior lobe of right lung was immediately removed and fixed in 4% formaldehyde in 0.01 M PBS (pH 7.4) for histopathological evaluation (Xu et al. 2015). Then the tissues were successively dehydrated in graded alcohols and embedded in paraffin. The paraffin sections (5 μm) mounted on glass slide were stained with hematoxylin and eosin (H&E) to observe the histopathological changes of lung under light microscopy 200 × magnification. Four pictures were randomly taken in each pathological section (n = 6) to measure the cell-covered area fraction (%) using the ImageJ system (Cheng et al., 2012). The area covered by cells was considered as “relative cell area”. The area except the major vein and lung hilum was considered as “overall area”. The cell-covered area fraction (%) = relative cell area / overall area × 100%.

*2.7. Measurement of the lung wet/dry weight ratio, the protein concentration, the total cells numbers, and the MPO activity in lung*

The inferior lobe of right lung of mouse was weighed immediately to acquire the “wet weight”, and then dried in an oven to constant weight to acquire the “dry weight”. Finally, the ratio of wet weight to dry weight was calculated, called wet/dry weight ratio (W/D ratio) (Xu et al. 2015).

The protein concentration and MPO activity in BALF were measured by BCA protein assay kit and MPO assay kit respectively according to the manufacturer's instructions. The total cell numbers in BALF were counted via a hemocytometer.

*2.8. Immunohistochemistry*

Immunohistochemical staining was performed as previously described (Xu et al., 2015). First, the high temperature antigen retrieval was carried out in the deparaffinized slide and the endogenous peroxidase was quenched. The non-specific binding sites of the sections were blocked with 5% BSA. Next, sections were incubated with rabbit monoclonal anti-TLR4 antibody (1:100) or rat anti-F4/80 antibody (1:100) overnight at 4 □ in a humid chamber. The next day, these sections were incubated with HRP-conjugated goat anti-rabbit or anti-rat IgG antibodies for 1 h at 37 □. Finally, the sections were visualized with the chromogenic substrate solution DAB and counterstained with hematoxylin. Then the sections were observed under light microscopy (Zeiss LSM 710). Four pictures were randomly taken in each pathological section (n = 6) and the average optical density (AOD) of positive area was measure by the ImageJ system (Chen et al., 2018). AOD = Integrated Optical Density (IOD) / Area.

*2.9. ELISA assay of the levels of TNF-α, IL-1β and IL-6 in BALF*

The levels of TNF-α, IL-1β and IL-6 in BALF were detected by mouse TNF-α, IL-1β and IL-6 ELISA kit according to the manufacturer's instructions.

*2.10. Western blot analysis*

Western blot analysis was performed as previously described (Feng et al., 2019). Ana-1 cells and lung tissues were treated in radio immunoprecipitation assay (RIPA) lysis reagent. Protein concentration was determined by the BCA protein assay kit. The protein samples were fractionated on 8% sodium dodecyl sulfate-polyacrylaminde gel electrophoresis (SDS-PAGE), blotted onto polyvinylidene difluoride (PVDF) membranes. After blocking with Tris-buffered saline and Tween 20 (TBST) containing 5% skim milk for 45 min at room temperature, the membranes were incubated overnight at 4 □ with the antibodies against TLR4, MyD88, TRAF6, phospho-NF-κB p65, NF-κB p65, iNOS, and β-actin (1:3000 dilution for TRAF6, 1:

1000 dilution for the others). On the next day, the membranes were washed three times with TBST, and then incubated with horseradish peroxidase (HRP)-conjugated IgG (1:2000 dilution) for 3 h. Afterwards, signals were detected by universal electrochemiluminescence (ECL) reagent and captured with a camera-based imaging system (Alpha Innotech, Santa Clara, CA, USA). The β-actin protein was served as internal control. The NF-κB p65 protein was served as reference of p-NF-κB p65.

*2.11. Statistical analysis*

Experimental data were presented as means ± standard deviation (S.D.). One-way analysis of variance (ANOVA) was performed for multiple group comparisons. If data were found to have significant changes, post-hoc comparisons were performed using Fisher's PLSD. $P < 0.05$ was regarded as statistically significant.

## 3. Results

*3.1. Effects of **5P39** on cell viability and inflammatory responses in vitro*

The peritoneal macrophages were isolated and cultured to evaluate the influences of **5P39** on cell viability, NO and IL-6 production. As shown in Fig. 2A, **5P39** had no adverse effect on cell viability with or without LPS stimulation. As shown in Fig. 2B and C, stimulations with LPS 1 μg/ml increased the levels of NO and IL-6 in the culture supernatants, and were significantly reduced with **5P39** treatment ($P < 0.05$). The **5P39** treatment alone had no effect on NO and IL-6 secretion compared with control group.

Ana-1 cells were incubated with **5P39** and LPS for 30 min or 24 h, then the cells were harvested to test the expression of key proteins in TLR4/MyD88 signaling pathway. As shown in Fig. 2D, **5P39** administration for 30 min significantly inhibited the expression of TLR4, TRAF6, iNOS and p-NF-κB p65 ($P < 0.05$), while the expression of MyD88 was not affected. As shown in Fig. 2E, **5P39** treatment for 24 h significantly reduced the expression of MyD88, TLR4, TRAF6 and iNOS ($P < 0.05$), but had no effect on the expression of p-NF-κB p65.

*3.2. Effects of **5P39** on the lung injury in LPS-induced ALI mice*

To assess the effects of **5P39** (30 and 60 mg/kg) on the lung injury in LPS-induced ALI mice, the histopathological changes of the lung tissues were detected. As shown in Fig. 3A, compared with the sham group, the lung tissues of the model group were characterized by thickening of the alveolar wall, interstitial hemorrhage, infiltration of neutrophils and macrophages, and edema. **5P39** (30 and 60 mg/kg) administration alleviated these symptoms. The results of semi-quantitative analysis also showed that the cell-covered area fraction of lung tissues in the model group was significantly increased, while **5P39** (30 and 60 mg/kg) treatment markedly inhibited the change.

To further evaluate the severity of lung edema, we measured lung wet/dry (W/D) ratio (Fig. 3B), a standard index of lung edema (Ye et al., 2019). Treatment of **5P39** markedly lowered the lung edema induced by LPS stimulation ($P < 0.001$).

As vascular leakage is a feature of ALI, we detected the protein concentration and the total cell number in BALF. As shown in Fig. 3C and D, compared with the sham group, the challenge of LPS to mice markedly upregulated the protein concentration and the number of total cells, while **5P39** obviously suppressed the LPS-induced damage ($P < 0.001$).

MPO activity, a reliable marker of polymorphonuclear neutrophil infiltration and activation (Ye et al., 2019), was also tested in this study. As shown in Fig. 4E, MPO activity in BALF increased dramatically after LPS administration. **5P39** (30 and 60 mg/kg) obviously inhibited the increasing MPO activity challenged by LPS ($P < 0.001$).

*3.3. Effects of **5P39** on the production of pro-inflammatory cytokines (TNF-α, IL-1β and IL-6) in BALF of LPS-induced ALI mice*

It was found that the levels of TNF-α (Fig. 4A), IL-1β (Fig. 4B) and IL-6 (Fig. 4C) in BALF were significantly upregulated after LPS instillation when compared with the sham group ($P < 0.01$). Administration of **5P39** clearly downregulated the secretion of these pro-inflammatory cytokines ($P < 0.05$).

*3.4. **5P39** attenuated TLR4 expression and inflammatory cells accumulation in lung tissues in LPS-induced ALI mice*

The effect of **5P39** on TLR4 expression and on the infiltration of macrophages (F4/80 expression) in lung tissues of mice was evaluated. The results showed intense immunostaining for TLR4 expression (Fig. 5A) and macrophages infiltration (Fig. 5B) in lung tissues of ALI model group. Compared with model group, ALI mice treated with **5P39** and DEX showed relatively low levels of staining in the lung tissues. The results of semi-quantitative analysis were consistent with the above observations.

*3.5. **5P39** inhibited the LPS-activated TLR4/MyD88 signaling pathway*

As shown in Fig. 6A, LPS instillation markedly increased TLR4 expression in lung tissues, whereas the increasing was inhibited by **5P39** (30 and 60 mg/kg) administration. As shown in Fig. 6 (B and C), in comparison to the sham group, LPS treatment dramatically upregulated the expression of MyD88 and TRAF6 in lung tissues, while **5P39** clearly suppressed the expression ($P < 0.05$).

Similarly, LPS obviously upregulated the expression of p-NF-κB p65 and iNOS (Fig. 6D and E) in lung tissues, whereas **5P39** (60 mg/kg) significantly inhibited the expression caused by LPS ($P < 0.01$).

## 4. Discussion

In this study, LPS stimulated an inflammatory like response in mouse peritoneal macrophages. The result of cell viability assay showed that **5P39** had no adverse effect on cell viability at the experimental concentration. In addition, the results of NO and IL-6 detection showed that **5P39** effectively inhibit the secretion of inflammatory mediators, indicating that **5P39** had obvious anti-inflammatory effect. **5P39** inhibited the overexpression of key proteins in TLR4/MyD88 signaling pathway when Ana-1 cells were stimulated with LPS for 30 min or 24 h. These results showed an interference of **5P39** with the immediate TLR4 signaling axis.

Based on the results of *in vitro* experiments, the anti-inflammatory effect and mechanism of **5P39** were further studied by establishing a mouse ALI model with

LPS. ALI is a common clinical problem with high morbidity and mortality in some emergency infectious diseases (Li et al., 2018; Jiang et al., 2018). Pulmonary edema, inflammatory cell infiltration and secretion of a large number of inflammatory cytokines are the main pathological features of ALI (Tan et al., 2018; Lin et al., 2019). In the present study, we found that **5P39** significantly suppressed lung W/D ratio, the protein concentration and the number of total cells in BALF. H&E staining results also showed that **5P39** administration clearly improved lung tissues hemorrhage, inflammatory cell infiltration and alveolar wall thickening caused by LPS. The above results indicated that **5P39** could obviously alleviate LPS-induced ALI.

During LPS-induced ALI, neutrophils are the earliest immune cells that are recruited to the site of inflammation and are essential for host defense (Grommes and Soehnlein, 2011; Peng et al., 2019). However, excessive activation of neutrophils leads to massive release of pro-inflammatory cytokines, destruction of the alveolar basement membrane, and formation of pulmonary edema (Peng et al., 2019; Zhang et al., 2018). MPO is an enzyme mainly found in neutrophils, which is proportional to the number of neutrophils in lung tissues and served as an indicator of neutrophil influx into tissues (Jiang et al., 2018; Niu et al., 2015). Experimental results demonstrated that LPS markedly upregulated the activity of MPO, while **5P39** observably inhibited the upregulation. Additionally, previous study suggested that pro-inflammatory cytokines such as TNF-α, IL-1β and IL-6 could activate neutrophils and macrophages accumulation, induce lung tissues injury, then lead to pulmonary edema (Zhao et al., 2017; Peng et al., 2019). After LPS challenge, TNF-α is considered to be the first to amplify the inflammatory response through triggering leukocyte activation and release of other factors (Li et al., 2018). IL-1β, another important pro-inflammatory cytokine, induces the production of secondary inflammatory cytokines (Veerdon et al., 2011). IL-6 promotes the release of vasoactive substances and neutrophils, causing a cascade of inflammation and aggravating tissues injury (Shin et al., 2015). Our study showed a beneficial effect of **5P39** on protecting against ALI by reducing these pro-inflammatory cytokines production, which were consistent with the results of the *in vitro* experiments.

Macrophages are widely distributed in various organs and tissues of the body, and are non-specific immune cells of the body. Macrophages have immunomodulatory effects such as antigen presentation and phagocytic necrosis (Benedetto et al., 2019). However, when the body is seriously infected and the inflammatory reaction in the tissues is too strong, the hyperactive macrophages release a series of inflammatory mediators and chemokines (Niesle et al., 2014). Subsequently, a large number of inflammatory cells such as neutrophils and macrophages adhere to the lung tissues, causing microcirculatory disturbances in the lungs and aggravating the occurrence of lung injury (Silva, 2010). F4/80 is a cell surface glycoprotein expressed in a variety of mature macrophages and is a mouse macrophage marker (Dos Anjos Cassado, 2017). In this study, the expression of F4/80 was detected in lung tissues by immunohistochemistry. Histopathological observation revealed that **5P39** significantly inhibited macrophages infiltration.

LPS has been reported to be a commonly used stimulator to induce ALI in mice (Lin et al., 2019). After invading the body, LPS bind to the specific receptor TLR4 on surface of cells such as macrophages and tracheal epithelial cells, which will lead to cells activation (Liu et al., 2019). Subsequently, a series of downstream adaptor proteins and protein kinases such as MyD88 and TRAF6 are activated, resulting in the activation of transcription factor NF-κB and the production of a large number of chemokines and inflammatory mediators, causing lung injury (Wang et al., 2019a; Zhang et al., 2018).

In the present study, it showed that LPS instillation resulted in a significant increase of TLR4 expression in lung tissue, **5P39** notably inhibited this increase. The testing results of key proteins in lung tissues revealed that **5P39** down-regulated the levels of TLR4, MyD88, TRAF6 and p-NF-κB p65 activated by LPS, suggesting that **5P39** might inhibit LPS-activated TLR4/MyD88 signaling pathway, which was consistent with the *in vitro* results. All these results showed that the anti-inflammatory effect of **5P39** might be related with down-regulating TLR4/MyD88 signaling pathway.

Furthermore, the expression of iNOS was investigated in lung tissue by Western

blot. Activation of the TLR4 signal arouses the expression of many genes associated with pre-immune and inflammation, such as iNOS (Hu et al., 2017; He et al., 2017). iNOS is one of the key enzymes catalyzes the production of NO from arginine in inflammatory reaction (Wang et al., 2017). NO, a short-lived gaseous signaling molecule, protects against invading pathogens and is therefore critical for the inflammatory response and innate immune system (Li et al., 2018; Cinelli et al., 2019). However, high level of NO is released into the blood circulation, stimulating inflammatory cell recruitment and activation in the ALI (Li et al., 2015). Besides, under pathological conditions, NO inhibits the $Na^+$ channel, thereby reducing the fluid transport capacity of alveolar epithelial cells, leading to pulmonary edema (Althaus et al., 2011). The experimental results displayed that the expression of iNOS in lung tissue was significantly increased in the LPS-induced group and clearly decreased after **5P39** treatment, which was consistent with the *in vitro* results. The results indicated that **5P39** might limit the secretion of NO by decreasing the expression of iNOS, thereby relieving lung injury caused by LPS.

DEX is a corticosteroid that is widely used in the treatment of various inflammatory diseases (Caceres-del-Carpio et al., 2016; Giuliano et al., 2012). It is also often selected as a positive control in the study of acute lung injury models (Xu et al., 2015; Xie et al., 2012). However, there are many adverse effects or limited therapeutic effects for the existing corticosteroids (Mokra et al., 2019). In this experiment, 5P39 showed a similar effect to DEX in improving LPS-induced lung injury and aimed to become an anti-inflammatory drug candidate in the future.

In conclusion, the present research showed that **5P39** significantly improved lung injury in LPS-induced ALI mice by relieving lung tissue edema, reducing inflammatory cells infiltration, and inhibiting excessive expression of inflammatory factors. The anti-inflammatory mechanism of **5P39** might relate to inhibition of the LPS-TLR4/MyD88 pathway. Consequently, **5P39** demonstrated a potential therapeutic agent for the treatment of ALI.

**Acknowledgments**

This work was supported by grants from National Natural Science Foundation of

China (21472025 and 21877015 to Y. W.; 81274165 to H. L.).

**Conflict of interests**

The authors declare that there are no conflicts of interest.

**Figure legends**

**Fig.1.** (A) The structures of *L*-cysteine, allicin and their conjugated derivatives. (B) The synthesis of compound **5P39**.

**Fig.2.** Effects of **5P39** on LPS-induced inflammation *in vitro*. Peritoneal macrophages were treated by **5P39** (5, 10, 20 μM) with or without LPS (1 μg/ml) stimulation for 24 h, then the cell viability (A) was detected by MTT assay and the culture supernatant was collected for NO (B) and IL-6 (C) detection. Ana-1 cells were treated by LPS (0.5 μg/ml) with or without **5P39** (20 μM) for 30 min (D) or 24 h (E), then the key proteins in TLR4/MyD88 signaling pathway were detected by Western blot. Data were expressed as means ± S.D., n = 3. $^{*}P < 0.05$, $^{**}P < 0.01$ and $^{***}P < 0.001$ compared with the control group, $^{\#}P < 0.05$, $^{\#\#}P < 0.01$ and $^{\#\#\#}P < 0.001$ compared with the LPS group, tested by the One-way ANOVA and the Fisher's PLSD.

**Fig.3.** Effects of **5P39** on the lung injury in LPS-induced ALI mice. Mice were administrated with vehicle (i.g.), **5P39** (i.g.), or DEX (4 mg/kg, i.v.) 2 h after instillation of NS or LPS (3 mg/kg). Lung sections were stained with H&E to observe the histopathological changes of lung under light microscopy 200 × magnification. The semi-quantitative analysis was done by measuring the cell-covered area fraction (A). The inferior lobe of the right lung was collected to get the lung W/D ratio (B). The protein concentration (C), the total cells numbers (D) and the MPO activity (E) in BALF were measured at 24 h after LPS challenge. Data were expressed as means ± S.D., n = 6. $^{*}P < 0.05$, $^{**}P < 0.01$ and $^{***}P < 0.001$ compared with the model group, tested by the One-way ANOVA and the Fisher's PLSD.

**Fig.4.** Effects of **5P39** on the production of pro-inflammatory cytokines (TNF-α, IL-1β and IL-6) in BALF of LPS-induced ALI mice. Mice were administrated with vehicle (i.g.), **5P39** (i.g.), or DEX 4 mg/kg (i.v.) 2 h after instillation of NS or LPS (3 mg/kg). The BALF was collected to detect the levels of TNF-α (A), IL-1β (B) and IL-6 (C) 24 h after LPS challenge. Data were expressed as means ± S.D., n = 6. $^{*}P <$

0.05, $^{**}P < 0.01$ and $^{***}P < 0.001$ compared with the model group, tested by the One-way ANOVA and the Fisher's PLSD.

**Fig.5. 5P39** attenuated TLR4 expression and inflammatory cells accumulation in lung tissues in LPS-induced ALI mice. Mice were administrated with vehicle (i.g.), **5P39** (i.g.), or DEX (i.v.) 2 h after instillation of NS or LPS (3 mg/kg). TLR4 expression (A) and macrophages infiltration (B) were detected by immunohistochemistry analysis under light microscopy 400 × magnification. The semi-quantitative analysis was done by measuring the AOD.

**Fig.6. 5P39** inhibited the LPS- activated TLR4/MyD88 signaling pathway and iNOS production. Mice were administrated with vehicle (i.g.), **5P39** (i.g.), or DEX 4 mg/kg (i.v.) 2 h after instillation of NS or LPS (3 mg/kg). Lung homogenates were prepared and analyzed by Western blot with antibodies specific to TLR4 (A), MyD88 (B), TRAF6 (C), p-NF-κB p65 (D) and iNOS (E). The β-actin protein was served as internal control. The NF-κB p65 protein was reference of p-NF-κB p65. Data were expressed as means ± S.D., n = 4. $^{*}P < 0.05$, $^{**}P < 0.01$ and $^{***}P < 0.001$ compared with the model group, tested by the One-way ANOVA and the Fisher's PLSD.

**References**

Althaus, M., Clauss, W.G., Fronius, M., 2011. Amiloride-sensitive sodium channels and pulmonary edema. Pulm Med. 2011, 830320. https://doi.org/10.1155/2011/830320.

Bellani, G., Laffey, J.G., Pham, T., Fan, E., Brochard, L., Esteban, A., Gattinoni, L., van Haren, F., Larsson, A., McAuley, D.F., Ranieri, M., Rubenfeld, G., Thompson, B.T., Wrigge, H., Slutsky, A.S., Pesenti, A., 2016. Epidemiology, patterns of care, and mortality for patients with acute respiratory distress syndrome in intensive care units in 50 countries. JAMA, 315(8), 788-800. https://doi.org/10.1001/jama.2016.0291.

Benedetto, P.D., Ruscitti, P., Vadasz, Z., Toubi, E., Giacomelli, R., 2019. Macrophages with regulatory functions, a possible new therapeutic perspective in autoimmune diseases. Autoimmun Rev, 102369. https://doi.org/10.1016/j.autrev.2019.102.

Caceres-del-Carpio, J., Costa, R.D., Haider, A., Narayanan, R., Kuppermann, B.D., 2016. Corticosteroids: Triamcinolone, Dexamethasone and Fluocinolone. Dev Ophthalmol, 55, 221-231. https://doi.org/10.1159/000431198.

Chen, M.Y., Li, H., Lu, X.X., Ling, L.J., Weng, H.B., Sun, W., Chen, D.F., Zhang, Y. Y., 2019. Houttuynia cordata polysaccharide alleviated intestinal injury and modulated intestinal microbiota in H1N1 virus infected mice. Chin J Nat Med, 17(3), 187-197. https://doi.org/10.1016/S1875-5364(19)30021-4.

Cheng, X.Q., Song, L.J., Li, H., Di H, Zhang, Y.Y., Chen, D.F., 2012. Beneficial effect of the polysaccharides from Bupleurum smithii var. parvifolium on "two-hit" acute lung injury in rats. Inflammation, 35(5), 1715-1722. https://doi.org/10.1007/s10753-012-9489-7.

Cinelli, M.A., Do, H.T., Miley, G.P., Silverman, R.B., 2019. Inducible nitric oxide synthase: Regulation, structure, and inhibition. Med Res Rev. 1-32. https://doi.org/10.1002/med.21599.

Dong, C., Wang, Y., Zhu, Y., 2009. Asymmetric synthesis and biological evaluation of Danshensu derivatives as anti-myocardial ischemia drug candidates. Bioorgan.

Med. Chem. 17(9), 3499-3507. https://doi.org/10.1016/j.bmc.2009.02.065.

Dos Anjos Cassado, A., 2017. F4/80 as a major macrophage marker: the case of the peritoneum and spleen, in: Kloc, M., Macrophages. Springer, pp. 161-179. https://doi.org/10.1007/978-3-319-54090-0_7.

Feng, Y., Weng, H., Ling, L., Zeng, T., Zhang, Y., Chen, D., Li, H., 2019. Modulating the gut microbiota and inflammation is involved in the effect of Bupleurum polysaccharides against diabetic nephropathy in mice. Int J Biol Macromol. 132, 1001-1011. https://doi.org/10.1016/j.ijbiomac.2019.03.242.

Freeman, F., Huang, B., Lin, R., 1994. Garlic Chemistry. Nitric Oxide Oxidation of S-2-Propenylcysteine and (+)-S-2-Propenyl-L-Cysteine Sulfoxide. J. Org. Chem. 59, 3227-3229. https://doi.org/10.1021/jo00090a048.

Giuliano, C., Smalligan, R.D., Mitchon, G., Chua, M., 2012. Role of dexamethasone in the prevention of migraine recurrence in the acute care setting: a review. Postgrad Med, 124(3), 110-115. https://doi.org/10.3810/pgm.2012.05.2554.

Gong, Q., Wang, Q., Pan, L., Liu, X., Xin, H., Zhu, Y., 2011. S-propargyl-cysteine, a novel hydrogen sulfide-modulated agent, attenuates lipopolysaccharide-induced spatial learning and memory impairment: involvement of TNF signaling and NF-kappaB pathway in rats, Brain Behav. Immun. 25(1), 110-119. https://doi.org/10.1016/j.bbi.2010.09.001.

Grommes, J., Soehnlein, O., 2011. Contribution of neutrophils to acute lung injury. Mol Med. 17(3-4), 293-307. https://doi.org/10.2119/molmed.2010.00138.

He, H.Q., Wu, Y.X., Nie, Y.J., Wang, J., Ge, M., Qian, F., 2017. LYRM03, an ubenimex derivative, attenuates LPS-induced acute lung injury in mice by suppressing the TLR4 signaling pathway. Acta Pharmacol Sin, 38(3), 342-350. https://doi.org/10.1038/aps.2016.141.

Hu, Y., Tao, L., Tan, H., Zhang, M., Shimizu, K., Zhang, F., Shimizu, K., Zhang, F., Zhang, C., 2017. An active drimane-type lactone from polygonum jucundum attenuates lipopolysaccharide-induced acute lung injury in mice through TLR4-MAPKs signaling pathway. Inflammation, 40(4), 1204-1213. https://doi.org/10.1007/s10753-017-0563-z.

Jia, Y., Dong, X., Zhou, P., Liu, X., Pan, L., Xin, H., Zhu, Y., Wang, Y., 2012. The synthesis and biological evaluation of novel Danshensu-cysteine analog conjugates as cardiovascular-protective agents. Eur. J. Med. Chem. 55, 176-187. https://doi.org/10.1016/j.ejmech.2012.07.016.

Jiang, X., Chen, L., Zhang, Z., Sun, Y., Wang, X., Wei, J., 2018. Protective and Therapeutic Effects of Engeletin on LPS-Induced Acute Lung Injury. Inflammation. 41(4), 1259-1265. https://doi.org/10.1007/s10753-018-0773-z.

Kashfi, K., Olson, K.R., 2013. Biology and therapeutic potential of hydrogen sulfide and hydrogen sulfide-releasing chimeras. Biochem. Pharmacol. 85(5), 689-703. https://doi.org/10.1016/j.bcp.2012.10.019.

Li, W., Zou, Z., Zhou, M., Chen, L., Zhou, L., Zheng, Y., He, Z., 2015. Effects of simvastatin on the expression of inducible NOS in acute lung injury in septic rats. Int J Clin Exp Pathol. 8(11), 15106-15111. https://doi.org/10.1007/s10114-012-0727-6.

Li, W., Zhao, R., Wang, X., Liu, F., Zhao, J., Yao, Q., Zhi, W., He, Z., Niu, X., 2018. Nobiletin-ameliorated lipopolysaccharide-induced inflammation in acute lung injury by suppression of NF-kappaB pathway in vivo and vitro. Inflammation, 41(3), 996-1007. https://doi.org/10.1007/s10753-018-0753-3.

Lin, Y., Qiu, D., Huang, L., Zhang, S., Song, C., Wang, B., Wu, J., Chen, C., 2019. A novel chalcone derivative, L2H17, ameliorates lipopolysaccharide-induced acute lung injury via upregulating HO-1 activity. Int. Immunopharmacol. 71, 100-108. https://10.1016/j.intimp.2019.02.002.

Liu, J., Chang, G.J., Huang, J., Wang, Y., Ma, N., Roy, A.C., Shen, X.Z., 2019. Sodium Butyrate Inhibits the Inflammation of Lipopolysaccharide-Induced Acute Lung Injury in Mice by Regulating the Toll-Like Receptor 4/Nuclear Factor κB Signaling Pathway. J Agric Food Chem. https://doi.org/10.1021/acs.jafc.8b06359.

Liu, X., Pan, L., Jia, Y., Wu, D., Xiong, Q., Wang, Y., Zhu, Y., 2013. A novel compound DSC suppresses lipopolysaccharide-induced inflammatory responses by inhibition of Akt/NF-κB signalling in macrophages. Eur. J. Pharmacol. 708,

8-13. https://doi.org/10.1016/j.ejphar.2013.01.013.

Matthay, M.A., McAuley, D.F., Ware, L.B., 2017. Clinical trials in acute respiratory distress syndrome: challenges and opportunities. Lancet Respir Med. 5(6), https://doi.org/10.1016/S2213-2600(17)30188-1.

Miron, T., Rabinkov, A., Peleg, E., Rosenthal, T., Mirelman, D., Wilchek, M., 2004. Allylmercaptocaptopril: a new antihypertensive drug. Am. J. Hypertens., 17(1): 71-73. https://doi.org/10.1016/S0895-7061(03)01035-5.

Miron, T., Listowsky, I., Wilchek, M., 2010. Reaction mechanisms of allicin and allyl mixed disulfides with proteins and small thiol molecules. Eur. J. Med. Chem., 45(5): 1912-1918. https://doi.org/10.1016/j.ejmech.2010.01.031.

Mokra, D., Mikolka, P., Kosutova, P., Mokry, J., 2019. Corticosteroids in Acute Lung Injury: The Dilemma Continues. Int J Mol Sci, 20(19). https://doi.org/10.3390/ijms20194765.

Niesler, U., Palmer, A., Radermacher, P., Huber-Lang, M.S., 2014. Role of alveolar macrophages in the inflammatory response after trauma. Shock, 42(1), 3-10. https://doi.org/10.1097/SHK.0000000000000167.

Niu, X., Wang, Y., Li, W., Mu, Q., Li, H., Yao, H., Zhang, H., 2015. Protective effects of Isofraxidin against lipopolysaccharide-induced acute lung injury in mice. Int Immunopharmacol, 24(2), 432-439. https://doi.org/10.1016/j.intimp.2014.12.041.

Pan, L., Liu, X., Zheng, H., Yang, H., Gong, Q., Zhu, Y., 2012. *S*-propargyl-cysteine, a novel hydrogen sulfide-modulated agent, attenuated tumor necrosis factoralpha-induced inflammatory signaling and dysfunction in endothelial cells, Int. J. Cardiol. 155(2), 327–332. https://doi.org/10.1016/j.ijcard.2011.12.059.

Pan, L., Liu, X., Jia, Y., Wu, D., Xiong, Q., Gong, Q., Wang, Y., Zhu, Y., 2013. A novel compound derived from danshensu inhibits apoptosis via upregulation of heme oxygenase-1 expression in SH-SY5Y cells. Biochimica et Biophysica Acta. 1830(4), 2861-2871. https://doi.org/10.1016/j.bbagen.2013.01.008.

Pan, L., Wang, J., Jia, Y., Zheng, H., Wang, Y., Zhu, Y., 2015. Asymmetric Synthesis and Evaluation of Danshensu-Cysteine Conjugates as Novel Potential

Anti-Apoptotic Drug Candidates. Int. J. Mol. Sci. 16(1), 628-644. https://doi.org/10.3390/ijms16010628.

Pandey, G.N., Rizavi, H.S., Bhaumik, R., Ren, X., 2019. Innate immunity in the postmortem brain of depressed and suicide subjects: Role of Toll-like receptors. Brain Behav Immun, 75, 101-111. https://doi.org/10.1016/j.bbi.2018.09.024.

Peng, L.Y., Yuan, M., Song, K., Yu, J.L., Li, J.H., Huang, J.N., Yi, P.F., Fu, B.D., Shen, H.Q., 2019. Baicalin alleviated APEC-induced acute lung injury in chicken by inhibiting NF-kappaB pathway activation. Int Immunopharmacol. 72, 467-472. https://doi.org/10.1016/j.intimp.2019.04.046.

Ren, Z., Li, H., Zhang, M., Zhao, Y., Fang, X., Li, X., Chen, W., Zhang, H., Wang, Y., Pan, L., Sun, J., 2018. A Novel Derivative of the Natural Product Danshensu Suppresses Inflammatory Responses to Alleviate Caerulein-Induced Acute Pancreatitis. Front. Immunol 9, 2513. https://doi.org/10.3389/fimmu.2018.02513.

Seetapun, S., Jia, Y., Wang, Y., Zhu, Y., 2013. Neuroprotective effect of Danshensu derivatives as anti-ischaemia agents on SH-SY5Y cells and rat brain. Biosci. Rep. 33 (4), e00062. https://doi.org/10.1042/BSR20130032.

Shin, N.R., Shin, I.S., Song, H.H., Hong, J.M., Kwon, O.K., Jeon, C.M., Kim, J.H., Lee, S.W., Lee, J.K., Jin, H., Li, W.Y., Oh, S.R., Hahn, K.W., Ahn, K.S., 2015. Callicarpa japonica Thunb. reduces inflammatory responses: a mouse model of lipopolysaccharide-induced acute lung injury. Int Immunopharmacol. 26(1), 174-180. https://doi.org/10.1016/j.intimp.2015.01.025.

Silva, M.T., 2010. When two is better than one: macrophages and neutrophils work in concert in innate immunity as complementary and cooperative partners of a myeloid phagocyte system. J Leukoc Biol. 87(1), 93-106. https://doi.org/10.1189/jlb.0809549.

Song, Z., Ng, M., Lee, Z., Dai, W., Hagen, T., Moore, P., Huang, D., Deng, L., Tan, C., 2014. Hydrogen sulfide donors in research and drug development. Med. Chem. Commun. 5, 557-570. https://doi.org/10.1039/C3MD00362K.

Tan, J., Li, L., Shi, W., Sun, D., Xu, C., Miao, Y., Fan, H., Liu, J., Cheng, H., Wu, M.,

Shen, W., 2018. Protective Effect of 2-Hydroxymethyl Anthraquinone from Hedyotis diffusa Willd in Lipopolysaccharide-Induced Acute Lung Injury Mediated by TLR4-NF-kappaB Pathway. Inflammation. 41(6), 2136-2148. https://doi.org/10.1007/s10753-018-0857-9.

van de Veerdonk, F.L., Netea, M.G., Dinarello, C.A., Joosten, L.A., 2011. Inflammasome activation and IL-1beta and IL-18 processing during infection. Trends Immunol, 32(3), 110-116. https://doi.org/10.1016/j.it.2011.01.003.

Wang, D., Wang, X., Tong, W., Cui, Y., Li, X., Sun, H., 2019a. Umbelliferone alleviates lipopolysaccharide-induced inflammatory responses in acute lung injury by down-regulating TLR4/MyD88/NF-kappaB signaling. Inflammation, 42(2), 440-448. https://doi.org/10.1007/s10753-018-00953-4.

Wang, G., Hu, Z., Fu, Q., Song, X., Cui, Q., Jia, R., Zou, Y., He, C., Li, L., Yin, Z., 2017. Resveratrol mitigates lipopolysaccharide-mediated acute inflammation in rats by inhibiting the TLR4/NF-kappaBp65/MAPKs signaling cascade. Sci Rep. 7, 45006. https://doi.org/10.1038/srep45006.

Wang, J., Fan, S. M., Zhang, J., 2019b. Epigallocatechin-3-gallate ameliorates lipopolysaccharide-induced acute lung injury by suppression of TLR4/NF-kappaB signaling activation. Braz J Med Biol Res. 52(7), e8092. https://doi.org/10.1590/1414-431X20198092.

Wu, J., Zhang, Y.Y., Guo, L., Li, H., Chen, D.F., 2013. Bupleurum polysaccharides attenuates lipopolysaccharide-induced inflammation via modulating Toll-like receptor 4 signaling. PLoS One. 8(10), e78051. https://doi.org/10.1371/journal.pone.0078051.

Xia, W., Luo, P., Hua, P., Ding, P., Li, C., Xu, J., Zhou, H., Gu, Q., 2019. Discovery of a New Pterocarpan-Type Antineuroinflammatory Compound from Sophora tonkinensis through Suppression of the TLR4/NFkappaB/MAPK Signaling Pathway with PU.1 as a Potential Target. ACS Chem Neurosci, 10(1), 295-303. https://doi.org/10.1021/acschemneuro.8b00243.

Xie, J.Y., Di, H.Y., Li, H., Cheng, X.Q., Zhang, Y.Y., Chen, D.F., 2012. *Bupleurum chinense* DC polysaccharides attenuates lipopolysaccharide-induced acute lung

injury in mice. Phytomedicine. 19(2), 130-137. https://doi.org/10.1016/j.phymed.2011.08.057.

Xu, Y.Y., Zhang, Y.Y., Ou, Y.Y., Lu, X.X., Pan, L.Y., Li, H., Lu, Y., Chen, D.F., 2015. *Houttuyniacordata Thunb.* polysaccharides ameliorates lipopolysaccharide-induced acute lung injury in mice. J Ethnopharmacol, 173, 81-90. https://doi.org/10.1016/j.jep.2015.07.015.

Yao, H., Sun, Y., Song, S., Qi, Y., Tao, X., Xu, L., Yin, L., Han, X., Xu, Y., Li, H., Sun, H., Peng, J., 2017. Protective Effects of Dioscin against Lipopolysaccharide-Induced Acute Lung Injury through Inhibition of Oxidative Stress and Inflammation. Front Pharmacol. 8, 120. https://doi.org/10.3389/fphar.2017.00120.

Ye, J.Y., Guan, M.Q., Lu, Y., Zhang, D., Li, C.Y., Li, Y.P., Zhou, C.C., 2019. Protective effects of hesperetin on lipopolysaccharide-induced acute lung injury by targeting MD2. Eur J Pharmacol. 852, 151-158. https://doi.org/10.1016/j.ejphar.2019.02.042.

Zhang, D., Li, X., Hu, Y., Jiang, H., Wu, Y., Ding, Y., Yu, K., He, H., Xu, J., Sun, L., Qian, F., 2018. Tabersonine attenuates lipopolysaccharide-induced acute lung injury via suppressing TRAF6 ubiquitination. Biochem Pharmacol. 154, 183-192. https://doi.org/10.1016/j.bcp.2018.05.004.

Zhang, T.Z., Yang, S.H., Du, J., 2014. The effects of morin on lipopolysaccharide-induced acute lung injury by suppressing the lung NLRP3 inflammasome. Inflammation. 37(6), 1976-1983. https://doi.org/10.1007/s10753-014-9930-1.

Zheng, Y., Yu, B., Cruz, L., Choudhury, M., Anifowose, A., Wang, B., 2017. Toward Hydrogen Sulfide Based Therapeutics: Critical Drug Delivery and Developability Issues. Med. Res. Rev. 38(1), 57-100. https://doi.org/10.1002/med.21433.

Zhao, G., Zhang, T., Ma, X., Jiang, K., Wu, H., Qiu, C., Guo, M., Deng, G., 2017. Oridonin attenuates the release of pro-inflammatory cytokines in lipopolysaccharide-induced RAW264.7 cells and acute lung injury. Oncotarget,

8(40), 68153-68164. https://doi.org/10.18632/oncotarget.19249.

Zhou, F., Zhang, Y., Chen, J., Hu, X., Xu, Y., 2016. Liraglutide attenuates lipopolysaccharide-induced acute lung injury in mice. Eur J Pharmacol. 791, 735-740. https://doi.org/10.1016/j.ejphar.2016.10.016.

Zhou, J., Deng, Y., Li, F., Yin, C., Shi, J., Gong, Q., 2019. Icariside II attenuates lipopolysaccharide-induced neuroinflammation through inhibiting TLR4/MyD88/NF-kappaB pathway in rats. Biomed Pharmacother. 111, 315-324. https://doi.org/10.1016/j.biopha.2018.10.201.

Zhu, X.S., Jiang, X.Y., Li, A., Zhao, Z.X., Li, S.Y., 2017. S□Allylmercaptocysteine Attenuates Cisplatin□Induced Nephrotoxicity through Suppression of Apoptosis, Oxidative Stress, and Inflammation. Nutrients, 9(2), 166. https://doi.org/10.3390/nu9020166.

**A**

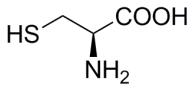


*L*-Cysteine

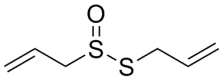


Allicin

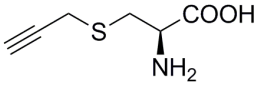


*S*-Propargyl-cysteine

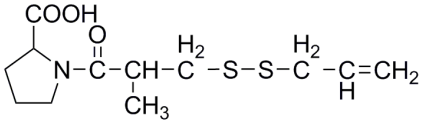


*S*-Allylthio-captopril

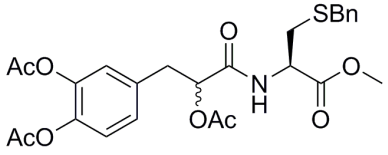


Danshensu-Cysteine Conjugate (DSC)

**B**